Supporting Information

The Synergy of Host-Guest Nonfullerene Acceptors Enables 16%-Efficiency Polymer Solar Cells with Increased Open-Circuit Voltage and Fill-Factor

Yuan Chang,[a,b,c] Tsz-Ki Lau,[d] Ming-Ao Pan,[a,b,c] Xinhui Lu,*[d] He Yan,*[c] and Chuanlang Zhan*[a,b]

[a] College of Chemistry and Environmental Science, Inner Mongolia Normal University, Huhhot 010022, China.

[b] Beijing National Laboratory for Molecular Sciences, CAS key Laboratory of Photochemistry, Institute of Chemistry, Chinese Academy of Sciences, Beijing 100190, China.

[c] Department of Chemistry, The Hong Kong University of Science and Technology, Clear Water Bay, Kowloon, Hong Kong, China.

[d] Department of Physics, Chinese University of Hong Kong, New Territories, Hong Kong, China.

[*] E-mail: clzhan@iccas.ac.cn (C.Z.), hyan@ust.hk (H.Y.), xinhui.lu@cuhk.edu.hk (X.L.)

Materials, methods, and characterizations

Materials. The materials of PBDB-T-SF, IT-4F, Y6, ITCT, PEDOT:PSS and PDINO were purchased from Solarmer company.

UV-Vis absorption spectra. Absorption spectra of donor polymers and acceptors in solid thin films were prepared by spin-coating their solutions atop the quartz glass substrates and measured on a Hitachi U-3010 UV−vis spectrophotometer.

Cyclic voltammetry measurements. For CV experiments, the compound was fully dissolved in N_2-degassed anhydrous $CHCl_3$ with a concentration of 10^{-4} M and then the solution was deposited onto the work electrode surface to form a thin solid film. CV traces were measured on an electrochemical workstation (CHI 660) at a scan rate of 50 mV/s using tetrabutylammonium tetrafluoroborate (Bu_4NBF_4) as the supporting electrolyte. A glassy carbon electrode, a Pt wire and an Ag/AgCl electrode were used as the working, counter and reference electrodes, respectively.

AFM characterizations. The AFM images were recorded using a Bruker multimode 8 AFM.

TFM characterizations. TEM experiments were performed on a JEM-2100 transmission electron microscope operated at 200 kV. For TEM experiments, the films were obtained by transferring the floated blend films from the water onto the Cu grid.

Solar cell fabrications and characterizations. Devices were fabricated on the Indium tin oxide (ITO) patterned glass with a conventional configuration of ITO/PEDOT:PSS/active layers/PDINO/Al. The ITO substrates with a sheet resistance of 10 ohm/square and transmission rate of 90% were firstly cleaned by detergent, deionized water, acetone and isopropanol in turn with sonication for 30 min respectively. The substrates were dried by nitrogen gas and then treated by UV-Ozone for 30 min before use. PEDOT:PSS was spin-coated onto the ITO substrates at 6000 rpm for 30 s, then the substrates were moved to oven and dried at 150°C for 15 min. The PBDB-T-SF:IT-4F:ITCT blends with different weight ratio were dissolved in chlorobenzene (CB) (the concentration of the donor was 7 mg/mL). This solution was stirred at 70°C for about 6 hours. Different ratios of DIO (0.50%, 0.75%, 1.00%) were added into the solution 30 minutes before device fabrication. The blend solution was spin-coated on the top of PEDOT:PSS layer followed by a thermal annealing step (80°C-10 min, 90°C-10 min, 100°C-10 min). The optimal method for active layer was to deposit the solution with 0.75% DIO at 2200 rpm and annealed at 80°C for 10 minutes. The PBDB-T-SF:Y6:ITCT blends with different weight ratio were dissolved in chloroform (CF) (the concentration of the donor was 5.5 mg/mL). This solution was stirred at 60°C for 4 hours. Different ratios of CN (0.25%, 0.50%, 0.75%, 1.00%) were added to the solution before device fabrication. The blend solution was spin-coated on the top of PEDOT:PSS layer followed by a thermal annealing step (80°C-10 min, 90°C-10 min, 100°C-10 min). The optimal method for active layer was to deposit the solution with 0.50% CN at 3000 rpm and annealed at 80°C for 10 minutes.

Atop the active layer, a thin electron transporting layer of PDINO (1.0 mg/mL in methanol, 3000 rpm for 30 s, about 15 nm) was spin-coated. Finally, the Al electrodes were thermally deposited on the top of devices, the thickness of which was about 90 nm. The current density-voltage (J-V) curves were measured in a nitrogen glove box and were conducted on a computer-controlled Keithley 2400 source measure unit under AM 1.5G (calibrated to be 100 mW/cm^2 with a reference silicon cell) using a solar illumination (AAA grade, XES-70S1). The EQE measurements were performed with the as-fabricated solar cell using a QE-R3011 instrument (Enli Technology Co. Ltd., Taiwan).

SCLC measurements. The electron and hole mobilities were measured by using the method called space-charge limited current (SCLC) for electron-only and hole-only devices. The structure of electron-only devices was ITO/titanium (diisopropoxide) bis(2,4-pentanedionate) (TIPD)[1]/active layer/PDINO/Al and the hole-only devices were fabricated with the structure of ITO/PEDOT:PSS/active layer/Au. The charge carrier mobility was determined by fitting the dark current to the model of a single carrier SCLC according to the Mott–Gurney law: $J = 9\varepsilon_0\varepsilon_r\mu V^2/8L^3$, where J is the measured current density, L is the film thickness of the active layer, μ is the mobility of charge carrier, ε_r is the relative dielectric constant of the transport medium component, and ε_0 is the permittivity of vacuum (8.85419×10^{-12} CV^{-1}m^{-1}), V is the difference of applied voltage (V_{app}) and offset voltage (V_{BI}). The mobility of charge carriers can be calculated from the slope of the $J^{1/2} \sim V$ curves.

GIWAXS measurements. GIWAXS data was carried out with a Xeuss 2.0 SAXS/WAXS laboratory beamline using a Cu X-ray source (8.05 keV, 1.54 Å) and Pilatus3R 300K detector. The incidence angle is 0.2°.

Supporting figures

Figure S1. Traces of cyclic voltammetry (CV) of PBDB-T-SF (a), IT-4F (b), Y6 (c), and ITCT (d) with ferrocene used as a reference.

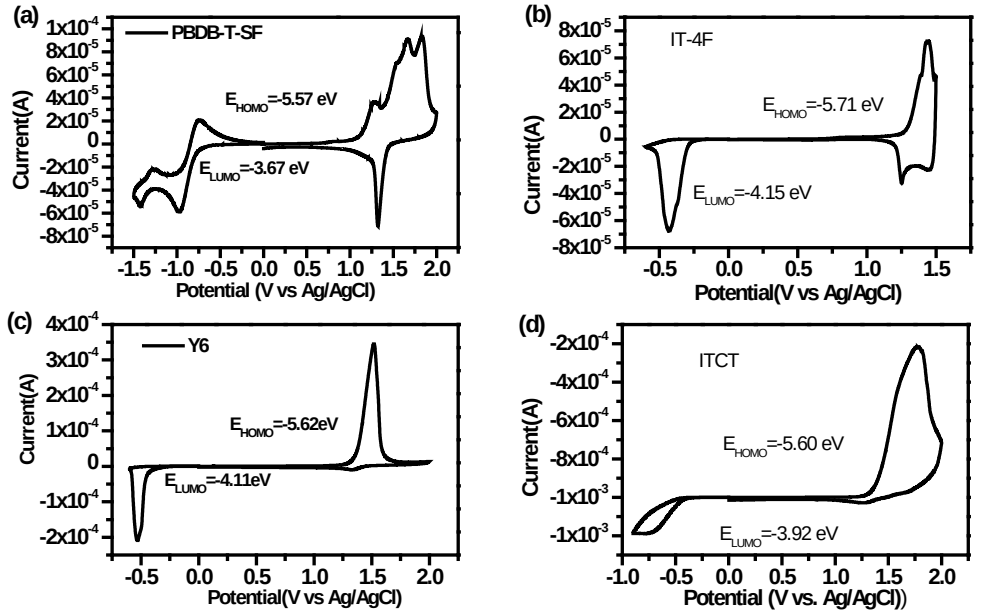

Figure S2. Traces of cyclic voltammetry (CV) of the mixtures of Y6:ITCT (a) and IT-4F:ITCT (b) with ferrocene used as a reference.

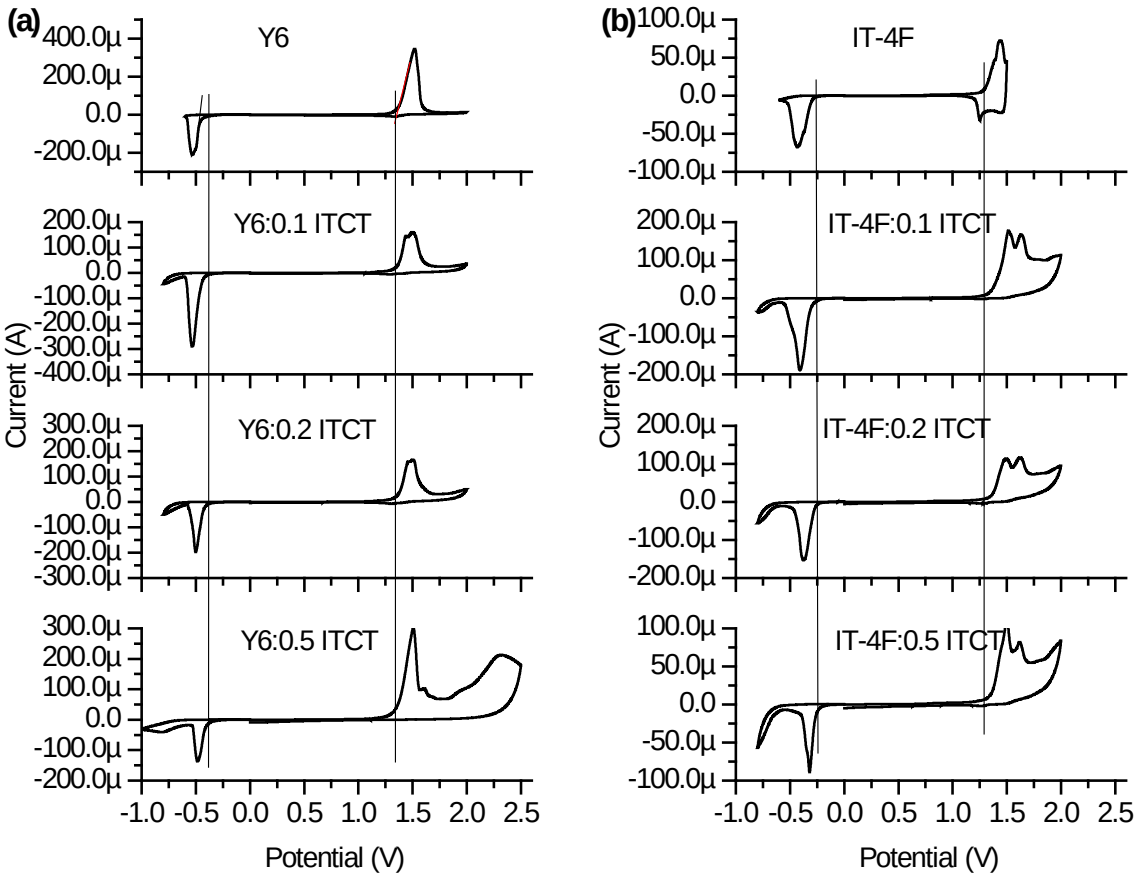

Figure S3. Scanning copy of the certificate report of a solar cell device with PBDB-T-SF:Y6:ITCT (1:1.1:0.1) as the active layer and PDINO as the ETL obtained from the National Institute of Metrology (NIM), China.

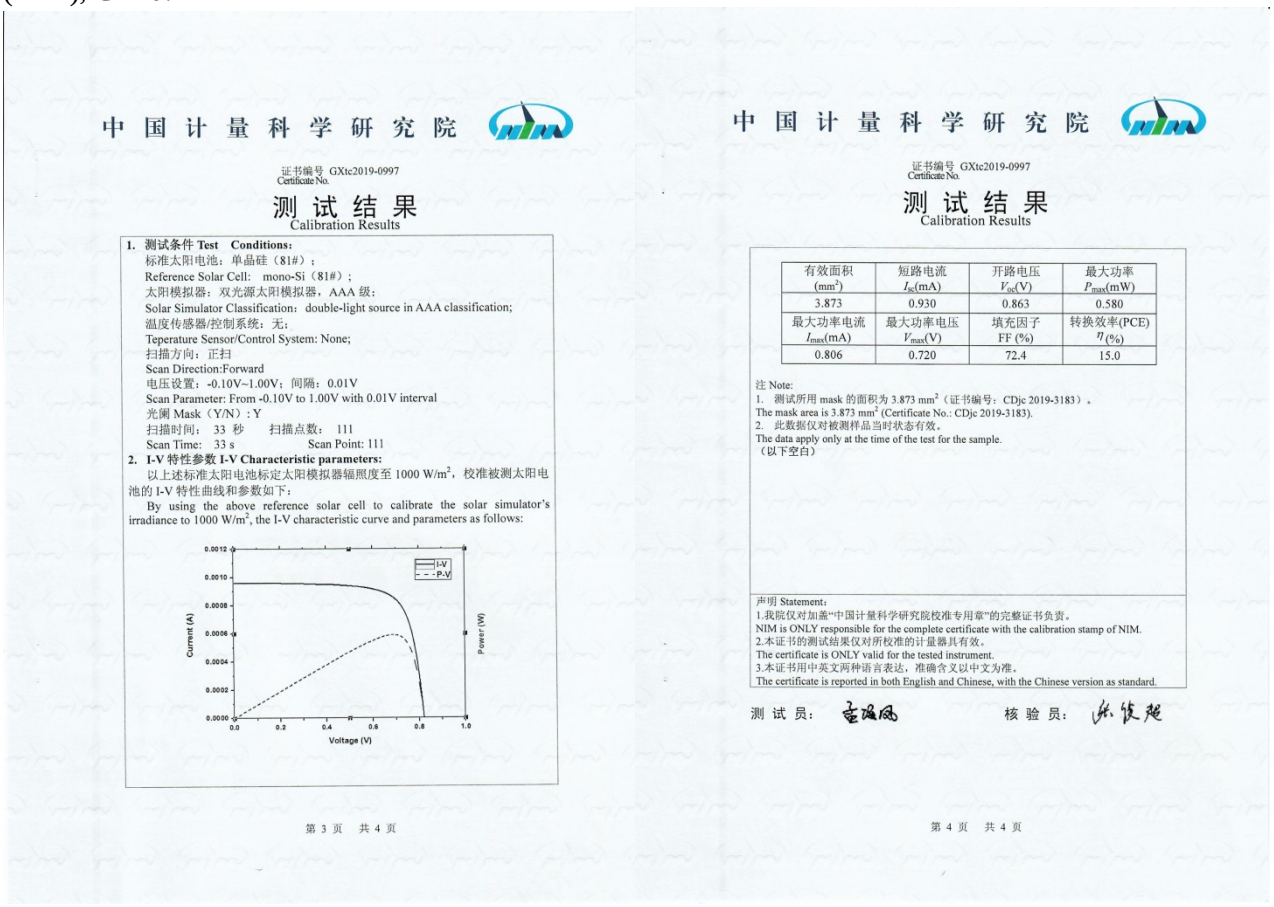

中 国 计 量 科 学 研 究 院

证书编号 GXtc2019-0997
Certificate No.

测 试 结 果
Calibration Results

1. 测试条件 Test Conditions:
标准太阳电池：单晶硅（81#）；
Reference Solar Cell: mono-Si（81#）；
太阳模拟器：双光源太阳模拟器，AAA 级；
Solar Simulator Classification：double-light source in AAA classification;
温度传感器/控制系统：无；
Teperature Sensor/Control System: None;
扫描方向：正扫
Scan Direction:Forward
电压设置：-0.10V~1.00V；间隔：0.01V
Scan Parameter: From -0.10V to 1.00V with 0.01V interval
光阑 Mask（Y/N）: Y
扫描时间： 33 秒 扫描点数： 111
Scan Time: 33 s Scan Point: 111

2. I-V 特性参数 I-V Characteristic parameters:
以上述标准太阳电池标定太阳模拟器辐照度至 1000 W/m^2，校准被测太阳电池的 I-V 特性曲线和参数如下：
By using the above reference solar cell to calibrate the solar simulator's irradiance to 1000 W/m^2, the I-V characteristic curve and parameters as follows:

第 3 页 共 4 页

中 国 计 量 科 学 研 究 院

证书编号 GXtc2019-0997
Certificate No.

测 试 结 果
Calibration Results

有效面积 (mm^2)	短路电流 I_{sc}(mA)	开路电压 V_{oc}(V)	最大功率 P_{max}(mW)
3.873	0.930	0.863	0.580
最大功率电流 I_{max}(mA)	最大功率电压 V_{max}(V)	填充因子 FF (%)	转换效率(PCE) η(%)
0.806	0.720	72.4	15.0

注 Note:
1. 测试所用 mask 的面积为 3.873 mm^2（证书编号：CDjc 2019-3183）。
The mask area is 3.873 mm^2 (Certificate No.: CDjc 2019-3183).
2. 此数据仅对被测样品当时状态有效。
The data apply only at the time of the test for the sample.
（以下空白）

声明 Statement:
1.我院仅对加盖"中国计量科学研究院校准专用章"的完整证书负责。
NIM is ONLY responsible for the complete certificate with the calibration stamp of NIM.
2.本证书的测试结果仅对所校准的计量器具有效。
The certificate is ONLY valid for the tested instrument.
3.本证书用中英文两种语言表达，准确含义以中文为准。
The certificate is reported in both English and Chinese, with the Chinese version as standard.

测 试 员： 核 验 员：

第 4 页 共 4 页

Figure S4. The $J^{0.5}$ – V plots for calculations of the electron (a and c) and hole (b and d) mobilities: IT-4F (a and b) Y6 based (c and d) binary and ternary blends.

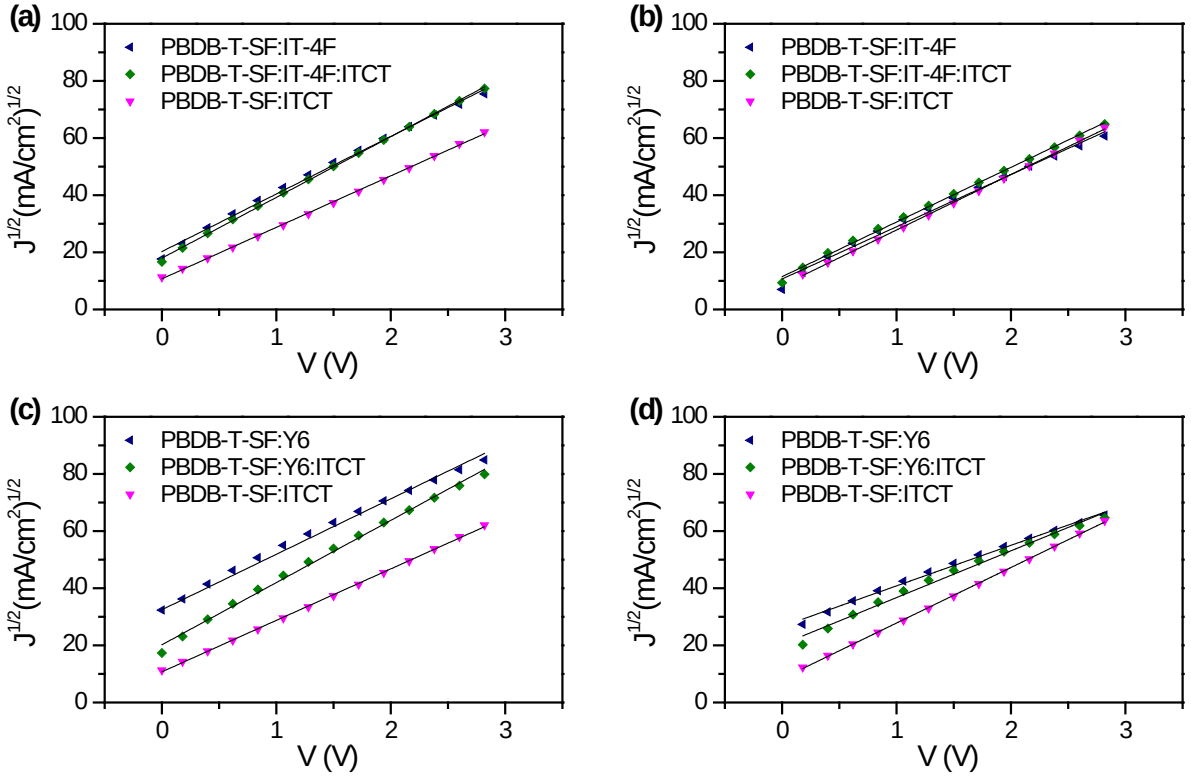

Figure S5. The plots of short-circuit current-density (J_{sc}) (a and c) and open-circuit voltage (V_{oc}) (b and d) vs. light intensity of the optimized binary and ternary devices: The IT-4F based (a and b) and the Y6 based (c and d).

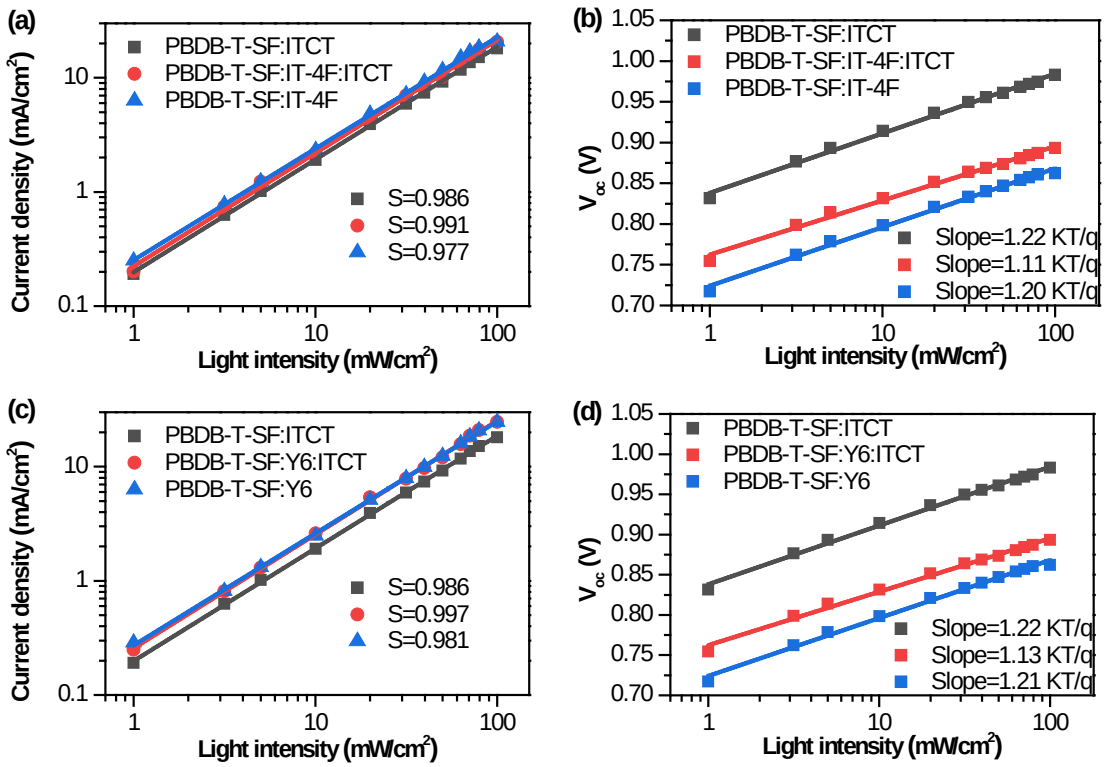

Figure S6. Photocurrent-density (J_{ph}) – effective voltage (V_{eff}) curves of the optimized binary and ternary devices: The IT-4F based (a) and the Y6 based (b).

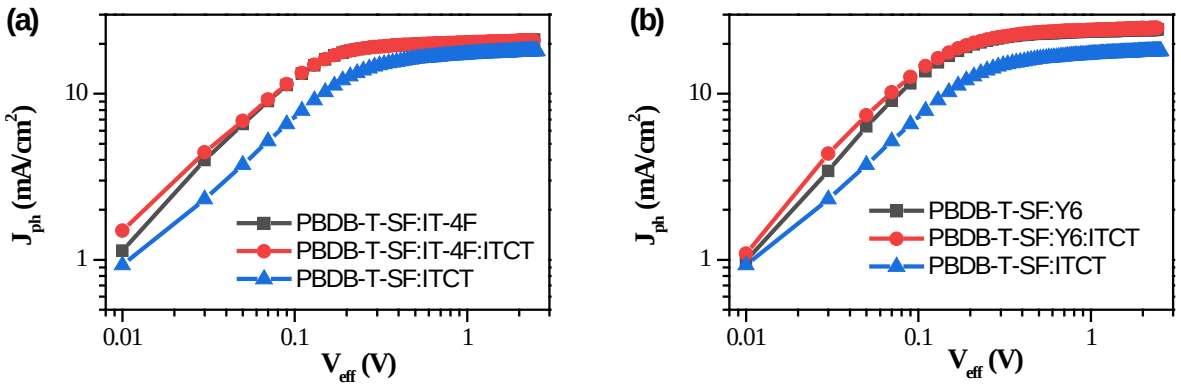

Figure S7. 2-D GIWAXS images (a-c) and the linecut profiles (d-f) of the neat ITCT (a and d), PBDB-T-SF (b and e), and Y6 (c and f) films, respectively.

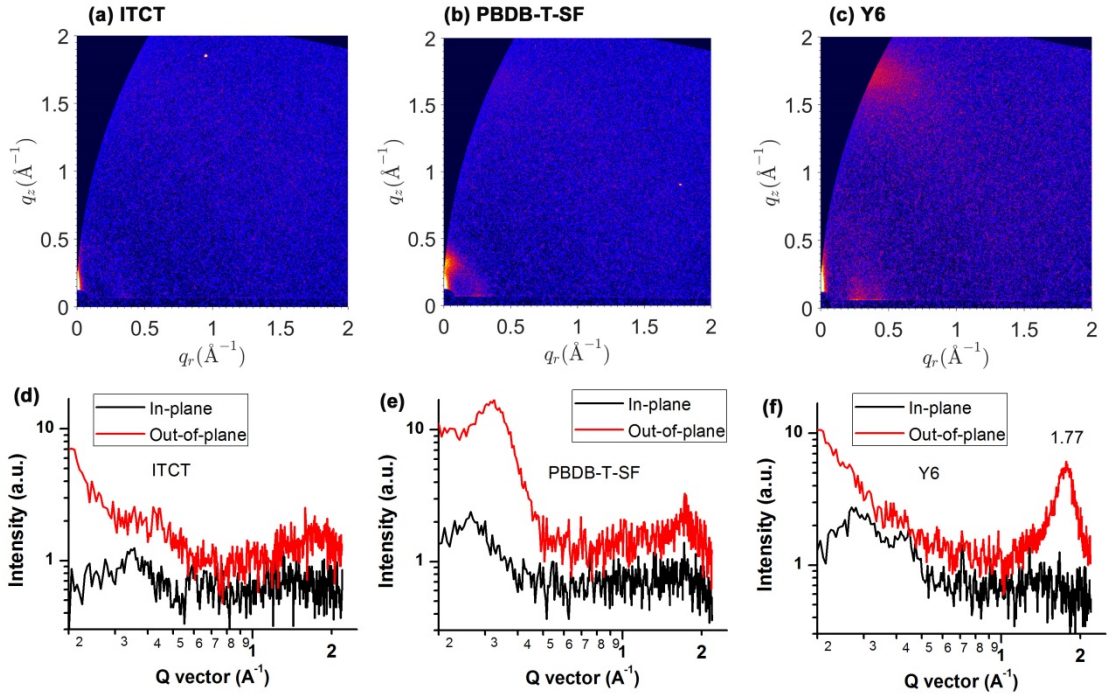

Supporting Tables

Table S1. The photovoltaic data of Y6 based binary and ternary solar cells with different optimized conditions.

Conditions		V_{oc} [a] [V]	J_{sc} [a] [mA/cm^2]	FF [a] [%]	PCE_{ave} [a] [%]
CN (%)	0.25	0.867 (0.863±0)	24.21 (19.06±0.15)	70.16 (69.24±1.58)	14.73 (14.41±0.24)
	0.50	0.864 (0.856±0)	24.68 (24.37±0.29)	71.19 (70.75±1.38)	15.18 (14.96±0.22)
	0.75	0.852 (0.847±0)	23.48 (19.69±0.21)	72.05 (71.84±1.36)	14.41 (14.15±0.17)
Annealing temperature (℃)	80	0.869 (0.862±0)	24.14 (24.00±0.17)	69.98 (69.25±1.45)	14.68 (14.39±0.20)
	90	0.864 (0.856±0)	24.68 (24.37±0.29)	71.19 (70.75±1.38)	15.18 (14.96±0.22)
	100	0.861 (0.855±0)	24.36 (24.14±0.14)	70.89 (70.27±1.42)	14.87(14.55±0.25)
Spin coating speed (rpm)	2700	0.860 (0.854±0)	25.14 (24.92±0.28)	70.13 (69.57±1.42)	15.16 (15.01±0.14)
	3000	0.864 (0.856±0)	24.68 (24.37±0.29)	71.19 (70.75±1.38)	15.18 (14.96±0.22)
	3300	0.867 (0.864±0)	24.16 (23.85±0.34)	71.35 (70.88±1.27)	14.95 (14.72±0.20)

Conditions		V_{oc} [a] [V]	J_{sc} [a] [mA/cm^2]	FF [a] [%]	PCE_{ave} [a] [%]
D:A ratio	1:1.2:0	0.864 (0.856±0)	24.68 (24.37±0.29)	71.19 (70.75±1.38)	15.18 (14.96±0.22)
	1:1.1:0.1	0.885 (0.880±0)	24.61 (24.21±0.20)	73.67 (72.39±1.42)	16.04 (15.83±0.18)
	1:1.0:0.2	0.897 (0.891±0)	23.49 (23.14±0.27)	71.46 (70.46±1.63)	15.06 (14.79±0.17)
	1:0.9:0.3	0.907 (0.901±0)	23.01 (22.25±0.22)	68.95 (67.97±1.58)	14.39 (14.07±0.21)
	1:0:1	0.981 (0.979±0)	18.11 (17.79±0.28)	61.45 (60.05±1.36)	10.92 (10.53±0.18)
CN (%)	0.25	0.887 (0.892±0)	23.95 (23.54±0.21)	71.46 (70.89±1.45)	15.18 (14.87±0.28)
	0.50	0.885 (0.880±0)	24.61 (24.21±0.20)	73.67 (72.39±1.42)	16.04 (15.83±0.18)
	0.75	0.881 (0.878±0)	23.46 (23.11±0.15)	72.37 (71.69±1.84)	14.96 (14.58±0.31)
Annealing temperature (℃)	70	0.891 (0.886±0)	24.23 (23.95±0.19)	71.15 (70.85±1.34)	15.36 (15.04±0.32)
	80	0.885 (0.880±0)	24.61 (24.21±0.20)	73.67 (72.39±1.42)	16.04 (15.83±0.18)
	90	0.879 (0.872±0)	24.04 (23.78±0.23)	73.39 (72.17±1.65)	15.51 (15.39±0.26)
Spin coating speed (rpm)	2700	0.880 (0.876±0)	25.01 (24.72±0.18)	71.47 (70.84±1.38)	15.72 (15.42±0.34)
	3000	0.885 (0.880±0)	24.61 (24.21±0.20)	73.67 (72.39±1.42)	16.04 (15.83±0.18)
	3300	0.889 (0.884±0)	23.96 (23.78±0.17)	73.95 (73.11±1.57)	15.75 (15.53±0.21)

Table S2. The photovoltaic data of IT-4F based binary and ternary solar cells with different optimized conditions.

Conditions		V_{oc} [a] [V]	J_{sc} [a] [mA/cm^2]	FF [a] [%]	PCE_{ave} [a] [%]
DIO(%)	0.25	0.868 (0.863±0)	19.21 (19.06±0.15)	69.79 (68.56±1.68)	11.64 (11.51±0.14)
	0.50	0.864 (0.858±0)	20.10 (19.57±0.19)	73.51 (72.49±1.59)	13.07 (12.91±0.18)
	0.75	0.861 (0.855±0)	19.86 (19.69±0.21)	72.46 (71.84±1.36)	12.09 (11.88±0.09)
Annealing temperature (℃)	80	0.869 (0.864±0)	20.27 (20.15±0.08)	71.97 (70.05±1.34)	12.68 (12.47±0.13)
	90	0.864 (0.858±0)	20.10 (19.57±0.19)	73.51 (72.49±1.59)	13.07 (12.91±0.18)
	100	0.860 (0.857±0)	19.85 (19.64±0.11)	71.46 (70.59±1.21)	12.20 (12.05±0.19)
Spin coating speed (rpm)	2000	0.861 (0.856±0)	20.51 (20.32±0.08)	71.53 (70.57±1.29)	12.63 (12.51±0.17)
	2200	0.864 (0.858±0)	20.10 (19.57±0.19)	73.51 (72.49±1.59)	13.07 (12.91±0.18)
	2500	0.868 (0.861±0)	19.76 (19.35±0.14)	74.09 (73.38±1.82)	12.71 (12.53±0.10)

Conditions		V_{oc} [a] [V]	J_{sc} [a] [mA/cm^2]	FF [a] [%]	PCE_{ave} [a] [%]
D:A ratio	1:1:0	0.864 (0.858±0)	20.10 (19.57±0.19)	73.51 (72.49±1.59)	12.77(12.31±0.18)
	1:0.9:0.1	0.888 (0.882±0)	20.19 (19.73±0.21)	76.23 (75.47±1.66)	13.67 (13.23±0.26)
	1:0.8:0.2	0.908 (0.903±0)	19.65 (19.13±0.24)	72.46 (71.89±1.23)	12.93 (12.49±0.07)
	1:0.7:0.3	0.913 (0.909±0)	19.01 (18.67±0.18)	69.95 (68.56±1.46)	12.14 (11.79±0.14)
	1:0:1	0.981 (0.977±0)	18.11 (17.79±0.28)	61.45 (60.05±1.36)	10.92 (10.53±0.18)
DIO (%)	0.5	0.898(0.892±0)	19.95 (19.79±0.19)	72.06 (71.89±1.37)	12.91 (12.57±0.08)
	0.75	0.888 (0.882±0)	20.19 (19.73±0.21)	76.23 (75.47±1.66)	13.67 (13.23±0.26)
	1	0.884 (0.878±0)	19.66 (19.26±0.17)	75..26 (74.39±1.57)	13.08 (12.88±0.09)
Annealing temperature (℃)	70	0.894 (0.889±0)	20.23 (20.05±0.08)	75.07 (74.58±1.25)	13.58 (13.23±0.12)
	80	0.888 (0.882±0)	20.19 (19.73±0.21)	76.23 (75.47±1.66)	13.67 (13.23±0.26)
	90	0.886 (0.881±0)	20.06 (19.74±0.11)	75.99 (74.79±1.32)	13.51 (13.35±0.18)
Spin coating speed (rpm)	2000	0.884 (0.879±0)	20.60 (20.52±0.08)	74.67 (73.69±1.39)	13.60 (13.31±0.12)
	2200	0.888 (0.882±0)	20.19 (19.73±0.21)	76.23 (75.47±1.66)	13.67 (13.23±0.26)
	2500	0.890 (0.884±0)	19.86 (19.67±0.14)	76.50 (75.12±1.62)	13.52 (13.23±0.10)

1. Z. Tan, W. Zhang, Z. Zhang, D. Qian, Y. Huang, J. Hou and Y. Li, *Adv. Mater.*, 2012, **24**, 1476-1481.